HYPERLOOP MANCHESTER

THE STUDENT-LED TRANSPORT REVOLUTION

MAGNETIC BRAKING SUB-SYSTEM

Final Showcase Document

HYPERLOOP MANCHESTER 2021/22

March 2022

Section B: Awards Application

Identify which systems you are applying for the Design Competition:

Award	Showcase [Y/N]	Demonstration [Y/N]	**Title of submission** (only one permitted, additional demonstrations in Section C)	**System Subcategories** (see Section A)	Page count in FSD/FDD
Mechanical Subsystem Award	Y	N	Hyperloop Manchester Magnetic Braking System	Braking System	28
Guiding Subsystem Award	N	N			
Traction Subsystem Award	Y	N	Hyperloop Manchester Magnetic Braking System	Braking System	
Electrical Subsystem Award	N	N			
Complete Pod Award	N	N			
Hyperloop Technology - Full-Scale Award	N	N			
Socioeconomic Impact – Full- Scale Award	N	N			

Section C: Additional Demonstrations

Identify which additional systems you are applying for showcase/demonstrate at EHW, outside the Design Competition. Add rows if necessary.

Title of submission	**System Category** (Mechanical, Guiding, Traction, Electrical, Complete Pod, Full Scale)	**System Subcategories** (see Section A)	**Showcase or Demonstration?**	**Page count in FSD/FDD**
N/A	N/A	N/A	N/A	N/A

Section D: Logistical Information

Identify the amount of power your team requires to demonstrate. Note that for every team during the demonstration two sockets (230V, ~10 Amps each) will be available. In the table below a request for more power can be made. Please note that European sockets (Type F) will be used and for power current (3/5 pins CEE).

Voltage	**Amperage required (16/32/...)**	**Amount of sockets**	**Is this required outside of the dedicated demonstration slot?* (Yes/No)**
230 V	N/A	N/A	N/A
400 V	N/A	N/A	N/A

Contents

1. Introduction

This document provides an overview of the Hyperloop Manchester team with regards to the internal work structure and the preparations for the EHW 2022 event. A general overview of the team is given first, explaining who we are, who are our team members, our values, and the development environment of Hyperloop Manchester.

The document then provides all necessary details on the specific hyperloop system to be registered for EHW 2022. The system in question is discussed, including the technical description, its size and components, the key features and elements, system integration and safety considerations.

2. Overview of the Team

This section describes Hyperloop Manchester in general, its values, and its development environment including research objectives. This section will provide the reader with a greater understanding of the core of Hyperloop Manchester and team principles.

2.1. Who Are We?

We are Hyperloop Manchester, a student-led team which aims to compete in international Hyperloop competitions organised by esteemed institutions and to share our knowledge with people around the world. The team was founded in 2019 and it has rapidly recruited a wide range of brilliant-minded members, from engineers to business students. We are gaining recognition globally year by year thanks to our business team. Now, Hyperloop Manchester has around 70 team members and around 50 alumni members from different nationalities and backgrounds.

The team consists of three main divisions: Technical, Research, and Business and Outreach. The Technical team consists of eight sub-teams, which themselves fall under three main categories: Mechanical, Electronics and Software. Members of the 2021/22 team are listed in the next section.

2.2. Team Members

Committee

Thomas Simpson
President

Rutvik Perepa
Chief Engineer

Luis Miguel Messias
Head of Business

Daiv Dalal
Head of Marketing

Abraham Levy
Head of Propulsion

Harry Shakesheff
Head of Power

Bassel Ezz
Head of Magnetic Braking

Karolis Gudziunas
Head of Suspension

Jaime Benthem
Head of Emergency Braking

Oliver Tunnicliffe
Treasurer

Tina Eslami
Technical Project Manager

Joel Chan
Head of Sponsorship

Ishaan Ghatak
Head of Electronics

Mikolaj Lenczewski
Head of Software

Akshat Damani
Head of Magnetic Levitation

James Ewing
Head of Chassis Integration

Jakub Zemek
Head of Outer Shell

Mechanical Team Members:

Propulsion

Abraham Levy
Head of Propulsion

Sunil Kumar
Propulsion Engineer

Abdallah Zakaria
Propulsion Engineer

Muhammad Raimi Bin Mohd Affandi
Propulsion Engineer

Yudhit Sharma
Propulsion Engineer

Konstantinos Margelos
Propulsion Engineer

Jean-Thomas Valls
Propulsion Engineer

Yousef Salama
Propulsion Engineer

Magnetic Levitation

Akshat Damani
Head of Magnetic Levitation

Yeshas Kuntamalla
Maglev Engineer

Ziad Ali
Maglev Engineer

Vaibhav Sharma
Maglev Engineer

Tibault Dary-Alabaster
Maglev Engineer

Adithya Vadakkadath
Maglev and Emergency Braking Engineer

Chassis Integration

James Ewing
Head of Chassis Integration

Merin Vallosseril
Chassis Integration Engineer

Jared Hassan
Chassis Integration Engineer

Hassan Shaker
Chassis Integration Engineer

Philip Rosborough
Chassis Integration Engineer

Afiq Iskandar Bin Md Zaid
Chassis Integration and Emergency Braking Engineer

Suspension

Karolis Gudziunas
Head of Suspension

Zhenhao Yang
Suspension Engineer

Giulio Stangarone
Suspension Engineer

Rokas Ramancevicius
Suspension Engineer

Afiq Nor Kamil
Suspension Engineer

Pascal Lai
Suspension Engineer

Daman Alam Sheikh
Suspension Engineer

Ignas Kurtinaitis
Suspension Engineer

Magnetic Braking

Bassel Ezz
Head of Braking

Llorenc Balada Gaggioli
Braking Engineer

Jai Singh Kurmi
Braking Engineer

Gary Zhang
Braking Engineer

Balint Macsuga
Braking Engineer

Mohamed Wael (Abdelsamad)
Braking Engineer

Brilliant Purnawan
Braking Engineer

Emergency Braking

Jaime Benthem
Head of Emergency Braking

Seungjoo Yang
Emergency Braking Engineer

Agamani Mullick
Emergency Braking Engineer

Tait Thompson
Emergency Braking Engineer

Harris Asghar
Emergency Braking Engineer

Outer Shell

Jakub Zemek
Head of Outer Shell

Irmak Keles
Outer Shell Engineer

Karim Elbehiri
Outer Shell Engineer

Muhammad Bin Saifullizan
Outer Shell Engineer

Mika Davies
Outer Shell Engineer

Jaikrishna Ramachandran
Outer Shell Engineer

Power

Harry Shakesheff
Head of Power

George Guthrie
Power Engineer

Seohee Jang
Power Engineer

Umar (Farooq) Khan
Power Engineer

Electronics and Software Team Members:

Electronics

Ishaan Ghatak
Head of Electronics

Fotis Kougionas
Electronics Engineer

Harry Heather
Electronics Engineer

Mohamed Hassan
Electronics Engineer

Software

Mikolaj Lenczewski
Head of Software

Andrei Popescu
Software Engineer

Lukas Rimkus
Software Engineer

Ashreen Kaur
Software Engineer

Lawrence Hunter
Software Engineer

Ivaylo Iliev
Software Engineer

Business Team Members:

Luis Miguel Messias
Head of Business

Daiv Dalal
Head of Marketing and Outreach

Ola Sztaborowska
Market Researcher and Social Media

Oliver Tunnicliffe
Treasurer

Joel Chan
Head of Sponsorship

Anish Shah
Sponsorship Analyst

Stepan Dishdishyan
Sponsorship Analyst

Tomáš Závodný
Rendering

Research Team Members:

Hakan Okten
Lead Researcher

Abraham Levy
Research Analyst

Oliver Tunnicliffe
Research Analyst

Llorenc Balada Gaggioli
Research Analyst

Team Advisors:

Hakan Okten
Co-Founder, Team Advisor and Lead Researcher

Batuhan Gerdan
Co-Founder and Team Advisor

2.3. Values

- **Diversity –** The team consists of around 70 members from multiple nationalities and different backgrounds. Hyperloop Manchester firmly believes that the key to the solutions of problems comes from different ideas which constitute diversity.
- **Teamwork –** This is the core of Hyperloop Manchester. Everything in Hyperloop Manchester is done with teams and collaboration. Teamwork along with efficient communication ensures that objectives are defined and reached successfully as we have been doing since the creation of Hyperloop Manchester.
- **Passion –** Everyone in Hyperloop Manchester is allocated in their teams according to their interests and passions. Therefore, every member is passionate about their involvement in the team, thus increasing productivity and a sense of accomplishment.
- **Creativity –** Tasks in the team are based on creative ideas and solutions to improve the aspects of the Hyperloop pod.
- **Innovation –** The essential value that describes the team is innovation. Hyperloop Manchester always aims to implement innovative applications in our designed Hyperloop pod and conduct research to continuously improve the Hyperloop structure.

2.4. Development Environment

During the global pandemic, Hyperloop Manchester swiftly and successfully shifted to the digital environment to ensure the safety of all their team members. Our day-to-day tasks include the use of Microsoft Teams to communicate, Google Drive to share files and engineering software environments, such as Autodesk, SolidWorks, and Altium Designer, to work on the design of our pod. Every week, we analyse the work done during that specific week, and we set the workload for the coming week.

Happily, post-lockdown the team have been able to move back to a primarily face-to-face working environment, whilst utilising the convenience and speed of online communication when applicable.

The development environment created by the members is also the learning environment. The team highly values the knowledge sharing internally and even externally. In the team, whenever the members have completed their main tasks, they are enthusiastic to develop themselves in the other areas that they are interested in. In doing so, this team spirit gives the members a prominent opportunity to explore their interests whilst they work and improve the pod.

The team has an interactive research scheme which is managed by the Research division inside the development environment. In the research segment, the team aims to collaborate with the University of Manchester regarding the Hyperloop-related research topics created by Hyperloop Manchester. The team is also in the process of initiating a research venture to investigate the application of graphene in a supercapacitor, in collaboration with Tufts University. Currently, the team is in standing communication with members of academic staff who are the supervisors of the team. Thanks to the created research topics and support of the team supervisors, the team is developing the pod design and can identify the spots which need to be improved easily. In addition to the scientific institutions of the University of Manchester, the Research division aims to enhance the Hyperloop-related research scope and to reach out to the people in other research institutions across the UK.

2.5. Representative and Design Competition Award

The team representative who is in charge of correspondence with the EHW Committee is Rutvik Perepa, with email perepa.rutvik@gmail.com.

Mechanical Subsystem Award

3. System

3.1. Introduction and Motivation

Brakes are a fundamental component of any moving vehicle. In the long term, our preferred method of braking is Eddy Current Brakes. We believe they are better than friction brakes for this application due to the fact that no contact with the track will be needed. The track is made of aluminium, which is very soft, making it harder to produce substantial braking forces without causing significant damage to the track. Friction brakes would also require more maintenance with repeated use which increases costs and the need for spare parts.

Therefore, we are in the process of designing a magnetic braking system, with the plan of finishing and building it by 2024.

Further description of the magnetic braking system will be discussed in the following sections.

3.2. Functionality and Theory

As previously explained, the desired functionality is to use magnets to brake. We use two magnet arrays that are on either side of the I-beam (track), they come into close proximity with the web of the I-beam which, because the pod (and thus the magnets), is moving relative to the I-beam, inducing eddy currents in the I-beam. These eddy currents consequently produce their own magnetic field which opposes the motion of the pod based on Lenz's law.

Specifically, halbach arrays will be used instead of regular alternating polarity arrays, as halbach arrays allow the magnetic field to be concentrated in the desired side of the array (in our case, the one that faces the I-beam), while the magnetic field on the opposite side is minimized [1] (Fig. 1).

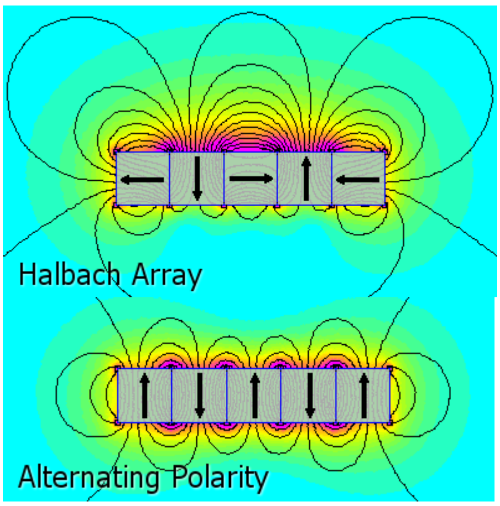

Figure 1. Magnetic field strength (indicated by colour scale) of a Halbach array vs Alternating polarity [1]

In terms of the physics behind the system's functionality, the equation for the flux density peak of the magnetic field generated by the halbach array is given by

$$B_0 = B_\mathrm{r} \left[\frac{sin(\pi/M)}{\pi/M}\left(1 - e^{-\mathrm{k\,dp}}\right)\right]$$ **(Eq. 1)** [2]

where Br is the remanent field of the magnets, M is the number of magnets per wavelength, which consists of magnets that complete a full rotation of its magnetization, k is the wavenumber $k = \frac{2\pi}{\lambda}$ and dp is the thickness of the magnets.

This has a directly proportional effect on the magnetic field in the relevant direction, that can be expressed as

$$B_\mathrm{y} = 2\, B_0\, e^{-k(\frac{ds}{2} + h)}\, cosh(ky)$$ **(Eq. 2)** [2]

where ds is the thickness of the I-beam, h is the gap between the magnets and the I-beam and y is the position of the magnets in the y-axis, which refers to the axis of the magnet movement.

Now, we can express the relevant component of the force generated by this field, which will be the effective drag force, given by

$$F_\mathrm{D} = C\, B_\mathrm{y}^2 \frac{\alpha}{(1+\alpha^2)}$$ **(Eq. 3)** [2]

where C contains some geometrical characteristics of the Halbach array and can be written as $C = \frac{w^2}{2\,k\,L}$, w is the width of the magnets and L the inductance, and α is a parameter given by $\alpha = \frac{R}{L\,k\,v}$, where R is the resistance and v is the velocity of the pod, and hence of the system.

These formulas were used in a self-developed Python script to produce all the plots shown in this document. Scripts can be provided on request from EHW.

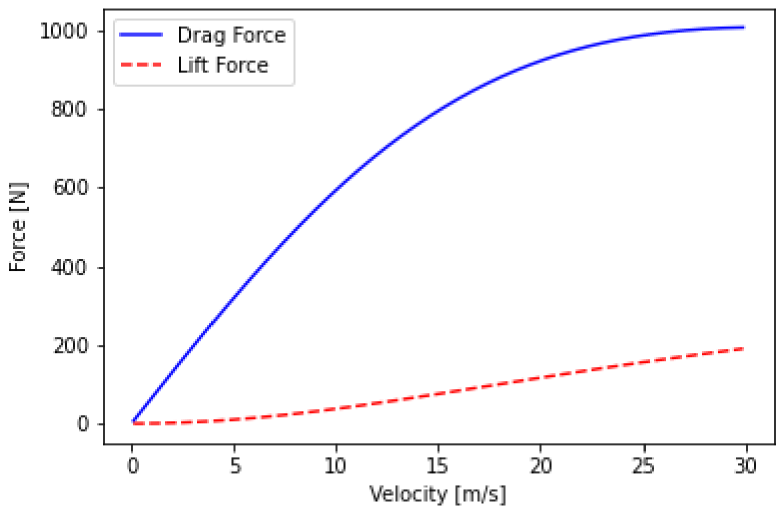

Figure 2. Python plot showing the braking force produced against pod velocity.

We can calculate the stopping distance numerically, by assuming constant acceleration between very small changes in velocity, from cruise speed down to 0 m/s.

$$s = \sum_{n=0}^{v_{max}} (u_{n+1}^2 - u^2) \ / 2a_n,$$

i.e break down the above acceleration (force / M) vs velocity graph into small sections (e.g. 0.001 m/s steps). Then calculate the distance to slow down 0.001 m/s, assuming constant acceleration in that small step. Then sum over all these distances from $u = 0$ to $u = v_{max}$, to find the total stopping distance. To increase precision, make the velocity step smaller.

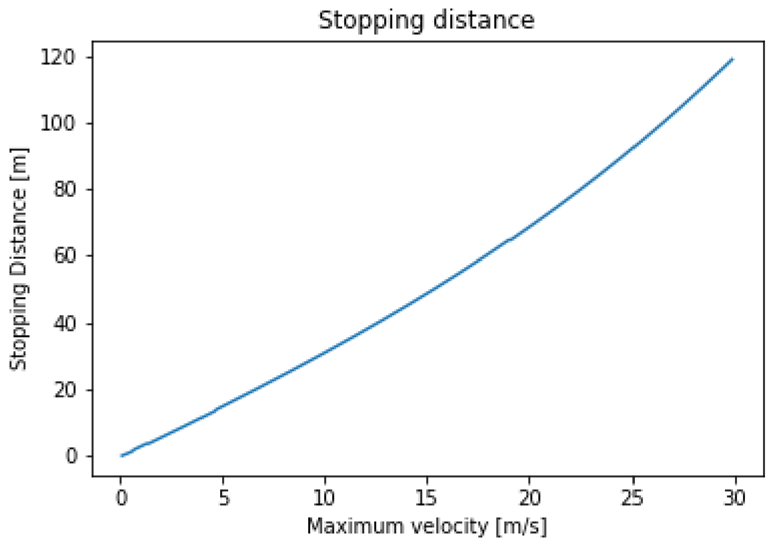

Figure 3. Python plot showing the pod stopping distance against pod velocity

Following all formulas above, we see that the force produced depends on the remanent field of the magnets. Therefore, the magnets used will be made from neodymium, which have high magnetic remanence. [6] Specifically, N50 grade will be used, which is one of the strongest Neodymium magnet grades [5].

From the formulas above (Eq. 1 & Eq. 3), we can see that the larger the size of the magnets, the larger the force generated. However, neodymium is a relatively heavy material, and having heavy arrays makes it harder to design a stable mechanical system that can move the magnets laterally closer to and away from the track. So, a compensation between braking force and stability & feasibility of the system has to be achieved.

For normal magnet arrays, a backing iron is used to focus the magnetic field on one side, and reduce it on the other side to shield other components from the magnetic effect. However, since halbach arrays are already designed to have that effect, a back iron is not required as the magnetic field strength on the non-desired sides would be negligible. [7] This means that we can reduce the mass of the array assembly by not using a backing iron case, and replacing it with a lighter and smaller aluminium plate.

Now we are going to vary the parameters to see the effect this would have on the braking forces and stopping distance.

1. Gap size between magnet array and I-beam

As shown by the formulas above (Eq, 1 Eq. 2 & Eq. 3), all the factors affecting the produced braking force are magnetic remanence (related to magnet type and grade chosen), dimensions of magnets, dimensions of track, relative velocity between magnets and track, material of the track, wavelength of the array, number of magnets in an array and the gap between magnets and track. Therefore, since all of these parameters except gap size will remain fixed after installation of the system, in order to vary the braking force, the gap between the magnet arrays and the track is varied (Eq. 2). When we want to engage the brakes, we move the magnet arrays closer to the I-beam (Fig. 10, Fig. 17), increasing the magnetic flux and, subsequently, braking force.

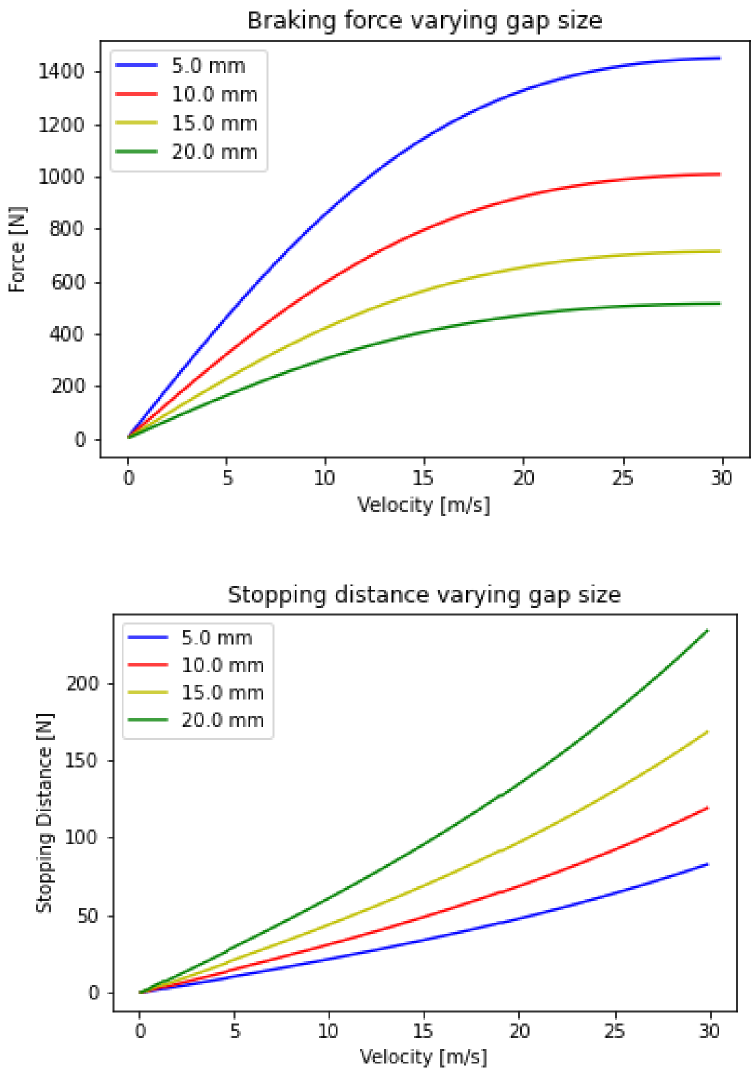

Figure 4. Python plot showing the braking force and stopping distance against pod velocity at various gap sizes

From this plot we can deduce that minimising the gap size will play a very important role in getting the maximum braking force we can, so it should be taken into account and prioritised. However, when the pod reaches very high velocities there are going to be vibrations and fluctuations on the distance that are going to be very hard to control so the smaller the gap size, the more risk the pod will be subject to as it will be easier to get in contact with the I-beam. This would be fatal for the system as it would destabilise the whole pod and probably produce damage and derailment. Therefore we see how the more we decrease the gap, the better force values we get with more difference, so the optimal value is between 10 mm and 5 mm, probably around 8 mm.

2. Number of magnets per array (per wavelength)

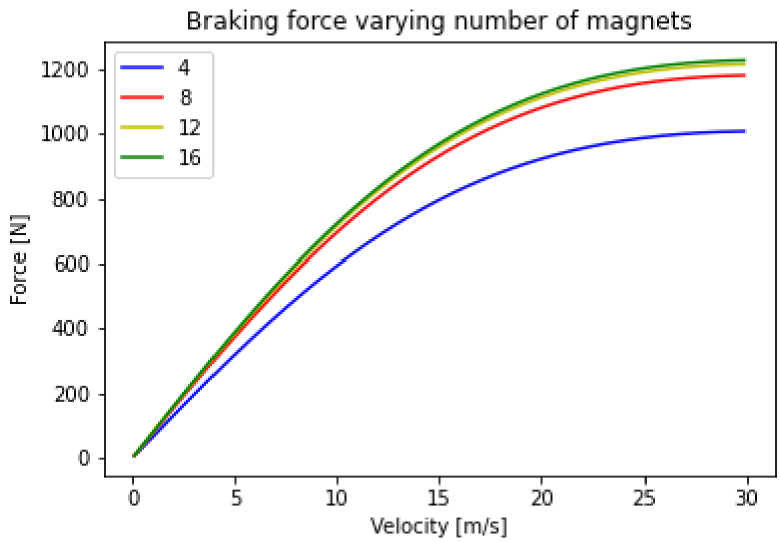

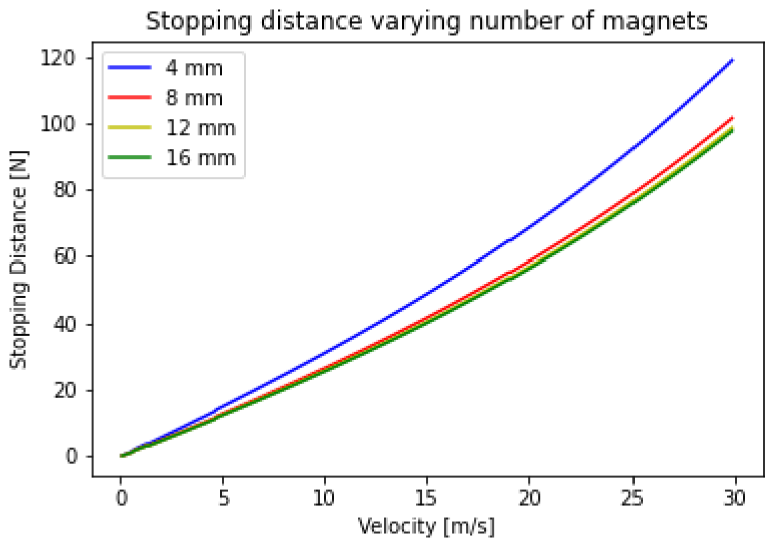

Figure 5. Python plot showing the braking force and stopping distance against pod velocity varying number of magnets per array

It can be seen now how varying the number of magnets per array (per wavelength) does not have that big impact on the braking force as the gap size did, so this parameter will be adjusted to fit the preference of the whole system and hence will probably be minimised so as to reduce the total weight and make manufacturing easier. After this consideration, we can say that the optimal amount of magnets is probably 4, due to the reduced force difference it provides to double the amount of magnets, to 8.

In a section later we will discuss how the number of wavelengths and the number of magnets affect the force and how by using the same number of magnets we can generate more braking force, so using different magnetization directions, which is the same as varying the number of wavelengths of the array. Although to do this we will need to propose different hypotheses to modify the braking force formula in accordance with the amount of wavelengths used, as the references only specify the force generated by one wavelength. At first sight it seems obvious that the braking force should be directly proportional to the number of wavelengths, but to prove this we have to test the system experimentally and/or use software like COMSOL to produce a simulation.

3. Thickness of magnets

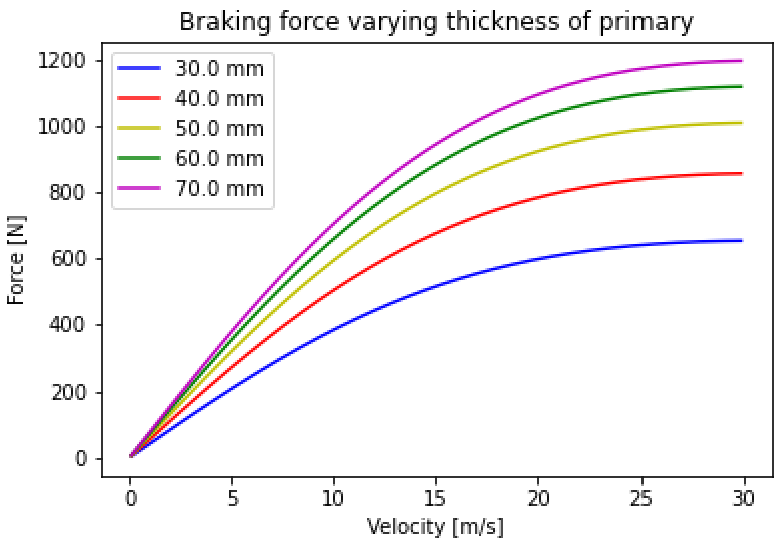

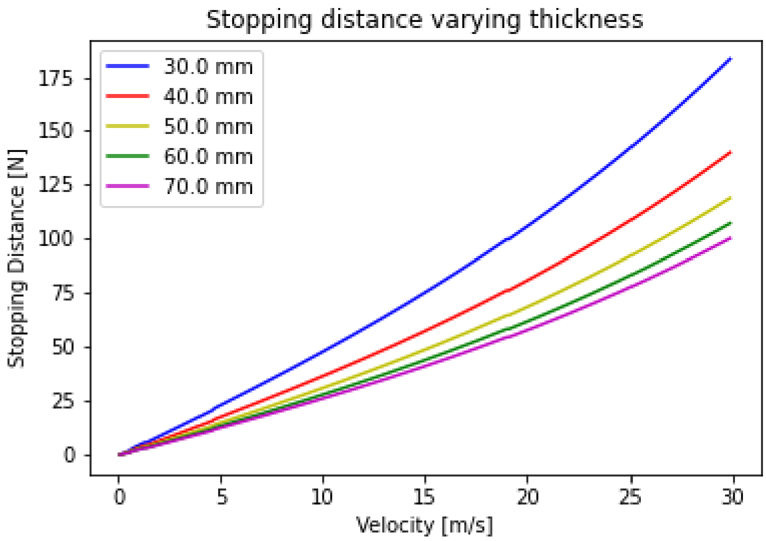

Figure 6. Python plot showing the braking force and stopping distance against pod velocity at various magnet thicknesses

We see from these two plots that the thickness of the magnets is a very important parameter with a very big influence on the braking force, which makes intuitive sense as the thickness plays a role in the area that of the magnets that will face the I-beam and hence if there is more area there will be more magnetic field increasing the force produced by the eddy currents, which are directly proportional to the intensity of the field.

Even if the more thickness the more force, we can also notice how, as in the other parameters, the difference is reduced the more we increase the thickness and so increasing further from 70 mm would not provide much improvement for the system probably, and it would increase the weight of the magnets in a proportional way, so the optimal value should be around 50 mm.

4. Wavelength

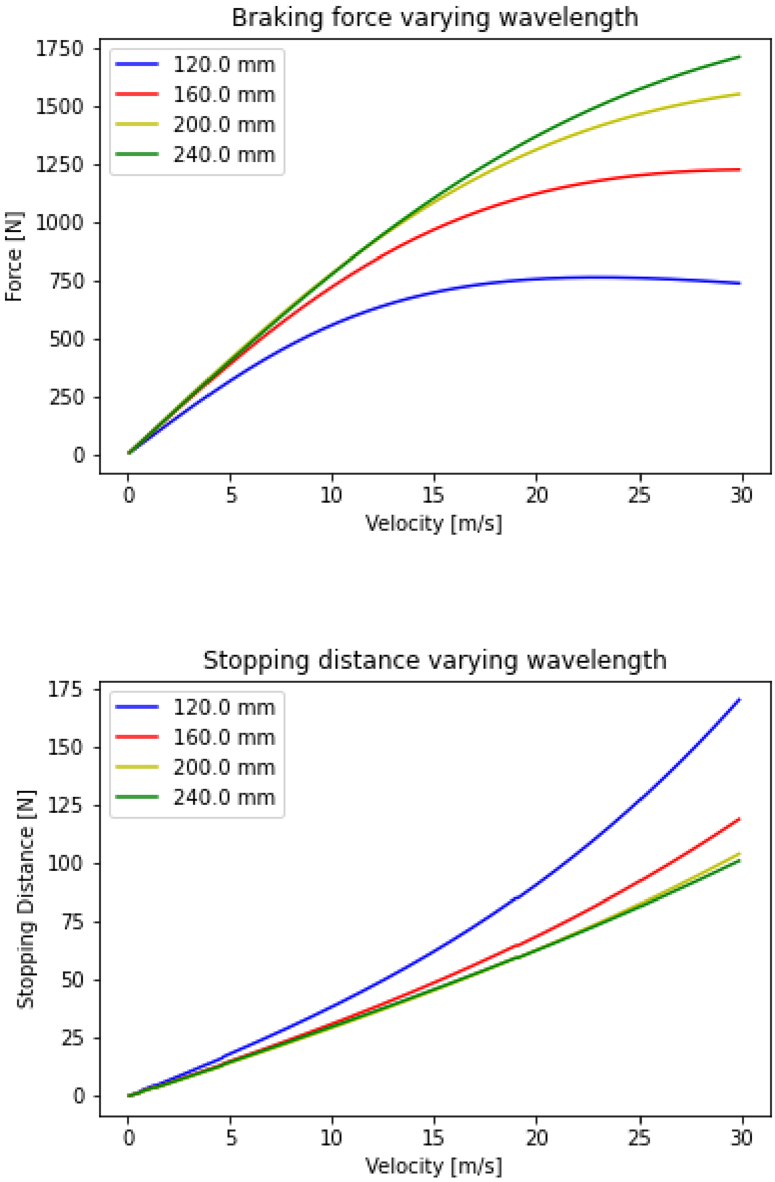

Figure 7. Python plot showing the braking force and stopping distance against pod velocity at various wavelengths

When plotting the varying wavelengths we see how we reach convergence at 240 mm, in the stopping distance plot specifically, which leads us to consider the optimal value of the wavelength to be 200 mm probably, also considering that if we have 4 magnets per wavelength we will have a magnet length of 50 mm, which would be the same as the thickness, although this factor doesn't play any important role as the magnets will be specifically manufactured with the required measures.

A thing we do have to consider is the space designated for the magnetic braking system when looking at the whole hyperloop pod, from which we can use 500 mm, so if we use a 200 mm wavelength we would be able to use 2 arrays, attached together and on each side of the I-beam, which would have a much greater impact on the braking force, although we still have to investigate the exact effect the increase of number of wavelengths will have on the force and stopping distances, which we will do after the plots of the results with the optimised parameters.

Force and stopping distance under optimised parameters

After the optimisation of the parameters from the plots of the different combinations of values for all the values we can change, we get to the conclusion that suitable parameters for the system would be the following:

Br = 1.46 T (Remanent magnetic field)
w = 50e-3 m (Width of magnets (primary))
dp = 50e-3 m (Thickness of magnets (primary))
ds = 10.46e-3 m (Thickness of I-beam (secondary))
wavelength = 200e-3 m (Wavelength)
h = 8e-3 m (Displacement gap)
m = 4 (Number of magnets per array)
L = 27.9e-9 H (Inductance)
R = 33.6e-6 Ω (Resistance)
M = 150 kg (Mass pod)

Where we have not only looked at the best parameters to use but also at the impact they would have on the system, as for example if we use sizes of the magnets that are too big, we would increase the weight of the array and therefore of the whole system too much, which would have a negative impact on other subsystems.

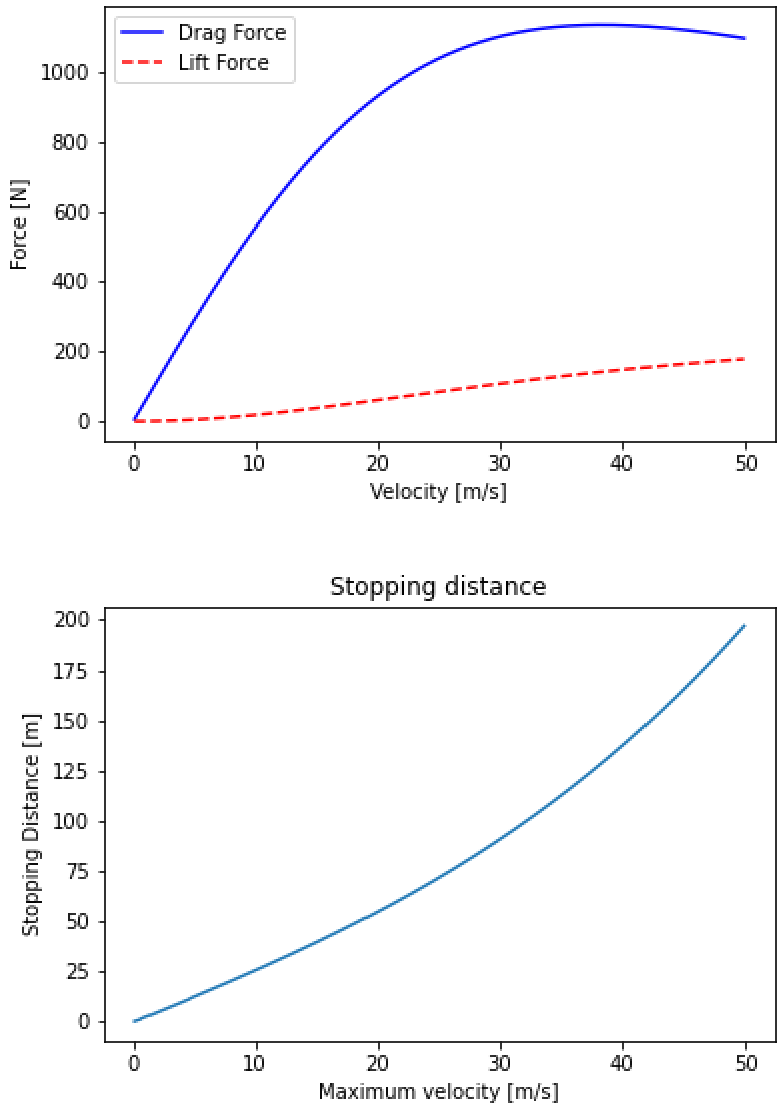

Figure 8. Python plot showing the braking force and stopping distance against pod velocity using optimal parameters

Force and stopping distance under hypothetical equation of force

How the increase of the number of wavelengths of the system will affect to the force or the stopping distance has to be determined experimentally or by the use of a simulation from a software package, so until we can produce a suitable simulation or we are able to reproduce the conditions to test a real braking scenario, we will hypothesise about how this effect will behave.

The first thing we can think of is a direct proportionality between the number of wavelengths and the braking force, so we will multiply the force by the number. Now, due to the limitations of space for the system, and considering the optimal wavelength is around 200 mm, we will produce the plots only for a system with 2 wavelengths, which is the maximum we would be able to have.

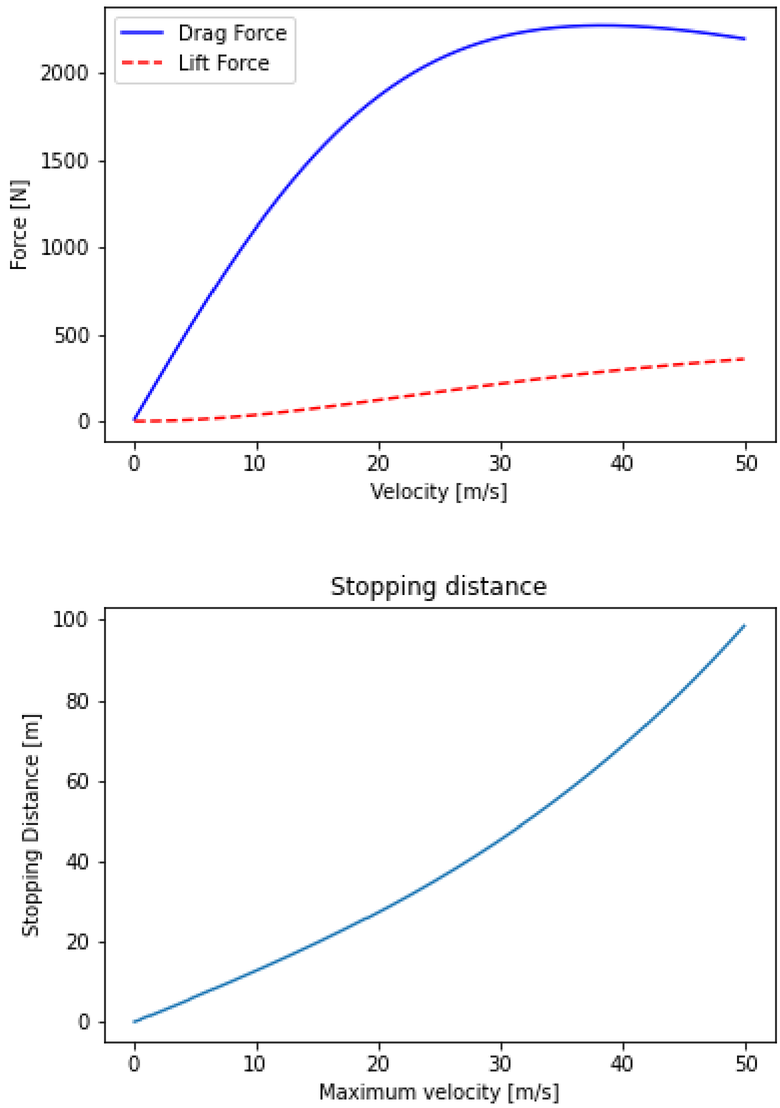

Figure 9. Python plot showing the braking force and stopping distance against pod velocity using optimal parameters and assuming linearity

As expected, we obtain values that are twice better compared to the previous plots, with numbers that produce a very good range of values for the system operation.

3.3. Design

3.3.1. Technical Description

Progress since the ITS submission has been held back by Christmas holidays and the university examinations. Therefore, we only had time to perform a critical review of our braking system. We identified some flaws that needed to be adjusted and came up with some concept designs that we believe correct these flaws. However, due to the time constraints mentioned above, we have not been able to finalise these designs in time before the FSD.1 submission deadline.

Therefore, only concepts will be briefly discussed in this section. In the meantime, the team is working hard to obtain more detailed sketches and CAD models of the full system comes the final FSD submission deadline.

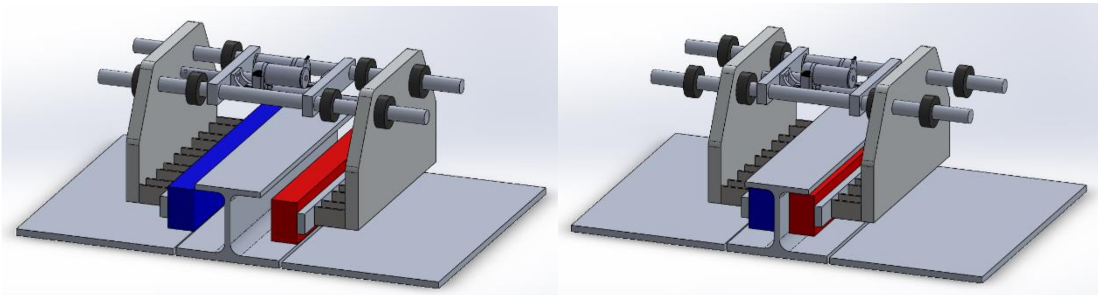

Figure 10. Overall appearance and layout of the old braking system assembly (Disengaged – Engaged)

Note: All CAD drawings are for illustrative purposes only and do not represent final assembly. Magnet arrays are represented as a single block.

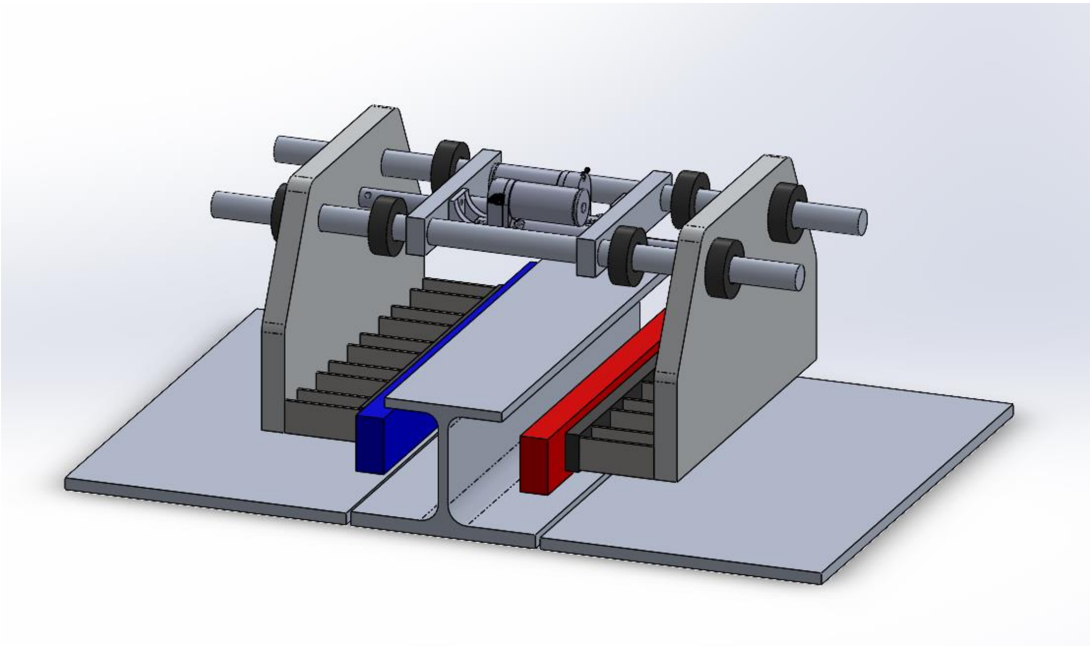

Figure 11. Old assembly

As seen above, (Fig.10, Fig. 11) many heavy components, such as side panels, magnets, and H-beams, had to be moved during the earlier installation of our braking mechanism. The weight of these components is supported by the chassis tubes, causing complicated bending moments. Furthermore, movement of the side panels during the application of brakes changes the bending moment across the chassis tubes. Thus, the application of brakes is problematic since it necessitates the movement of heavy components. Additionally, due to space limits, actuator placement is a problem. The actuators must be installed and supported in between chassis tubes, increasing the system's overall instability. The magnet arrays were attached to the side panels using a cantilever beam, which makes it hard to control any vibrations that the magnets may experience as the braking forces are applied. The system was suspended from the chassis tubes and had no more supports, which makes swinging a concern with pod vibrations.

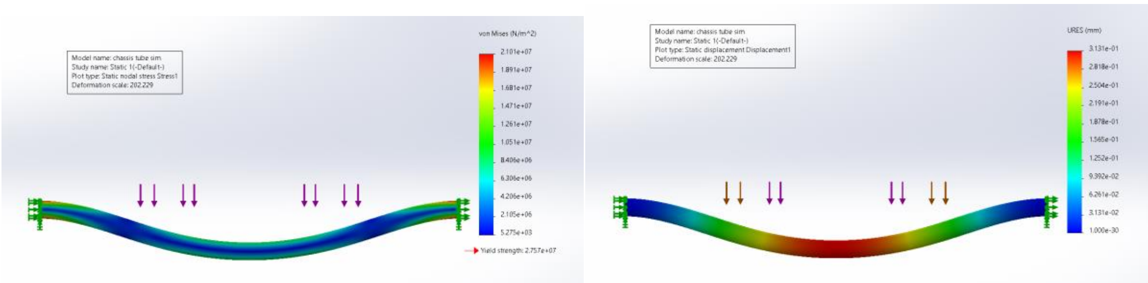

Figure 12. Stress analysis on Chassis tube

The issues described could be solved by constructing a truss structure, which is attached to the lower part of the chassis, that serves solely to support the magnets. This truss structure will support a table, which will be supported by linear roller bearings for the magnet engagement mechanism. This table can simply be suspended beneath the chassis with a suspension mechanism built to absorb unwanted vibrations during operations.

We have boiled down to 3 possible engagement mechanisms which are:

1) Rack and pinion engagement mechanism: The magnets are engaged and disengaged using a rack and pinion mechanism. The motor/actuators are mounted on the lower section of the chassis, above the supporting table. After that, the motor drives the pinion, which drives the rack, which engages the brakes. This arrangement is two on each side. The rack is positioned on top of the table/platform, which is supported by the truss structure built beneath the chassis. To make translation easier, the rack glides over the linear roller bearings on a guide. In order to balance the weight of the magnet on one end, the rack is also fastened through the guide.

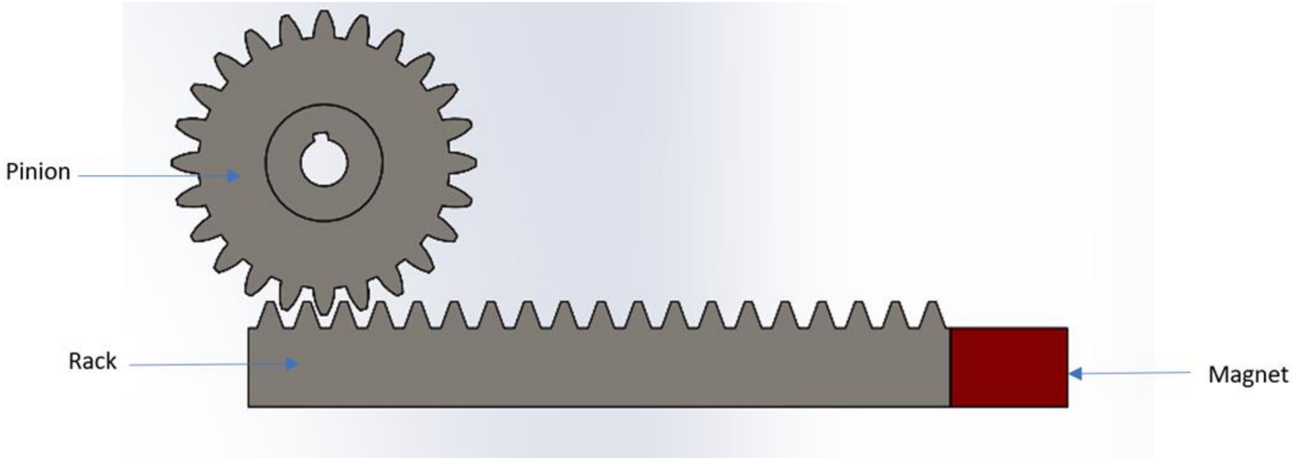

Figure 13. Rack and pinion

2) Double rack and pinion mechanism: The internal rack of the double rack and pinion system is powered by a pinion with midway gears. The pinion extends and engages the break on half rotation, then retracts and disengages the brakes on the other half rotation. A motor/actuator drives the pinion, via direct drive or reduction through chain or gearing drive, and such a system can be utilised on both sides. In the horizontal plane, the pinion engages with the rack and is supported by the platform/table, which is supported by the truss framework. The rack slides over a slider supported by linear roller bearings over the horizontal truss support from the chassis in this system.

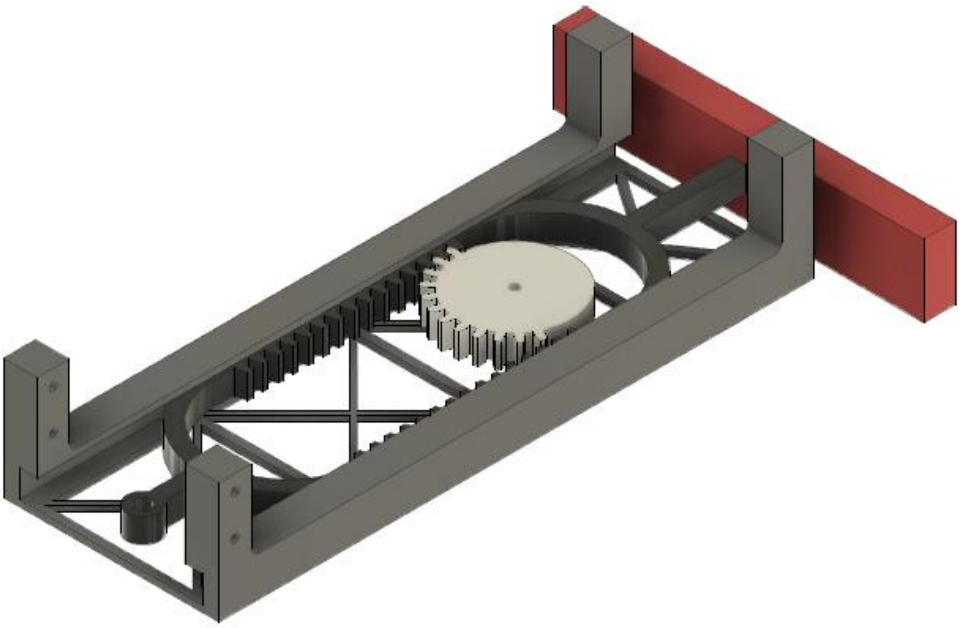

Figure 14. Double rack and pinion

3) Lead Screw: The lead screw configuration can also be used for brake engagement. An electric motor drives the lead screw, and the truss structure supports the weight. The lead screw's ends are joined by a bearing that is mounted vertically from the chassis. These screws hold the nut that is attached to the magnets, allowing the magnets to translate and engage and disengage the brakes as the lead screw rotates. The nut should support the magnets on both ends on a side, hence there should be two lead screw mechanisms on each side. The lead screw is driven by a motor via a chain drive or geared in the vertical plane.

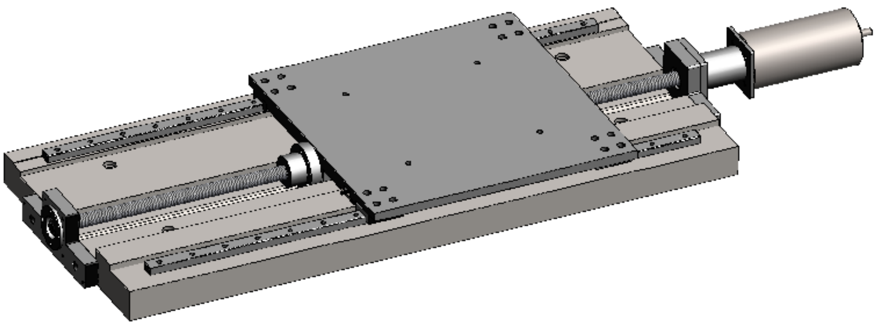

Figure 15. Lead screw mechanism example

Due to budget constraints, the magnetic braking system is not going to have a real life model by the start of the European Hyperloop Week (EHW). Hence, only CAD drawings, simulation and testing results, as well as the testing prototype will be presented at the EHW.

3.3.2. Design Constraints and Considerations

At Hyperloop Manchester, we have opted for using a safety factor of 3 for all mechanical components and systems.

After communication with other subsystems, a target top speed of 100 kph (27.78 m/s) was agreed.

For calculations of stopping distance, the weight of the pod has been estimated to be 150 kg.

Our original design was to have two magnet arrays on each side of the flange of the I-beam to maximize the braking force (Fig. 16). However, the space above the flange needs to be reserved for the Maglev (Magnetic levitation) system. So we moved our arrays to be on both sides of the I-beam web (Fig. 17). We also therefore have to lift our chassis tubes a distance of 70 mm above the I-beam to leave enough space for the Maglev skis.

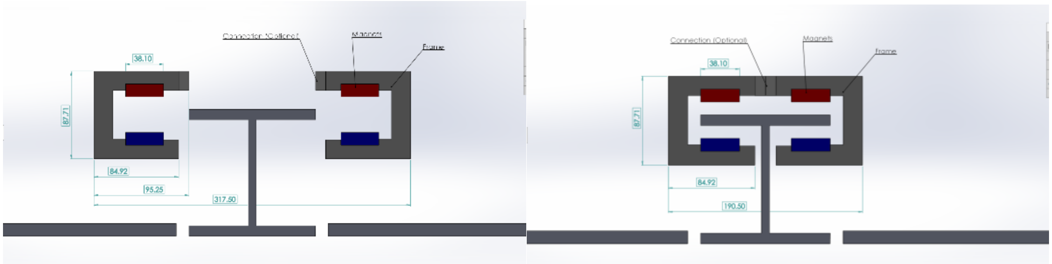

Figure 16. Initial magnet array layout on flanges

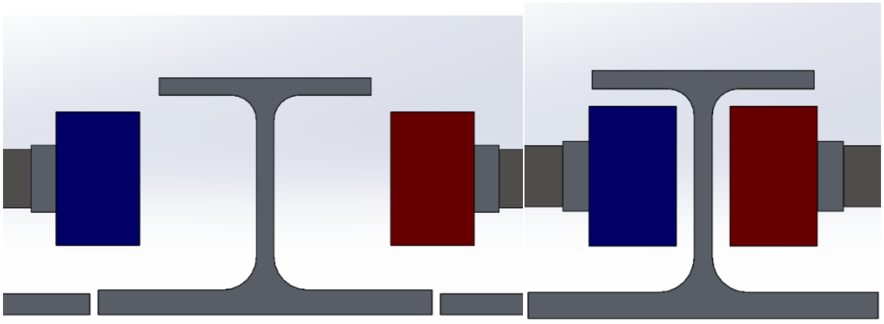

Figure 17. Current magnet array layout on web

Our pod uses a passive Maglev system (i.e. levitating height cannot be controlled and is only dependent on pod velocity). This means that as the pod slows down due to braking, the pod will start to descend. In our case, this descent is calculated to be 10 mm, after that the take-off wheels would come in contact with the top of the I-beam preventing any further descent. According to EHW rules, there are specified keep-out zones above the bottom flange of the I-beam where our magnets are not allowed to go. This was therefore considered when choosing our magnet dimensions to make sure that after the drop due to braking, our magnets would still be outside the keep-out zones.

The magnetic braking system was allocated £300 for miniature prototype testing purposes, which will be covered with more detail later in section 3.4.

3.4. Testing

For even further validation, testing of the braking theory is planned and will be conducted to obtain real-life data of braking force against velocity. The results of this will be compared to the analytical and simulated solution.

Only the magnetic braking will be tested, not the engagement system. This is because the engagement system is currently undergoing a redesign and budget constraints mean that we would not be able to build and test it by the start of EHW.

However, Altair software will be used to perform the finite element analysis on the components of the system to make sure they can withstand all the stresses and forces inflicted on them. This is an iterative process where the design will be updated, and exact material choice will be confirmed as we proceed with the analysis.

Testing will be performed on an aluminium I-beam track of similar dimensions to that provided in the rules for EHW. A pneumatic launching mechanism will be used to launch the prototype along the track. The system will use a pressurized chamber, which coupled with a quick exhaust valve (QEV) allows for a large amount of air to be release in a very short time, due to the QEVs short activation time, which provides a greater impulse and hence gives the cart a higher initial acceleration.

The magnets used for testing will be 10x10x10 mm cubes. Since the testing cart will be a lot lighter than the pod and will travel at a lower velocity, these magnets should be sufficient.

An Inertial Measurement Unit (IMU) will be used to collect velocity and acceleration data from the test launches. These will be compared to the analytical solution at a range of initial velocities and number of wavelengths to test our assumption of linearity.

We will be performing the tests at speeds ranging from $5\ m/s$ to $10\ m/s$. Relevant data that will be collected and plotted is stopping distance at various speeds, and variation of braking force with velocity. To test the assumption that the braking force will vary linearly with the number of wavelengths used, we will repeat all tests using one, two and three wavelengths.

To reduce complexity of the testing cart, it will not contain an engagement mechanism for the brakes. Meaning the magnet arrays will be in close proximity with the I-beam at launch. Therefore, we will be using a steel I-beam section with low magnetic properties of similar dimensions to the testing I-beam at the start of the track. The idea is to give the testing cart time to accelerate and reach the intended velocity before reaching the aluminium section and braking forces start to become significant.

The testing cart will be brought to EHW to help explain the testing arrangement. However, the car will not be put into motion.

3.5. Safety Concerns

Gap size: When considering the optimal value of the gap size between the I-beam and the halbach arrays, we observe that the less gap size the more braking force, and also the higher increase of it. However, we have to take into account vibrations and fluctuations of the stability of the pod, which would be a high risk if the gap size was too low, so if we take this into account we should maintain a bigger gap size in order not to affect the safety of the pod and decrease the risk of having arbitrary contacts with the I-beam, which would destabilise the entire pod. Moreover, any engagement or disengagement of any parts of the system will make the pod move so we should determine how much the different mechanical operations make the pod get closer to the I-beam so as to increase the gap size accordingly to maintain an adequate level of safety.

Low speed scenario: From the plots produced we have seen how the stopping distance increases exponentially, which means that at low velocities stopping distances will not decrease fast enough to make the pod reach a null velocity in an appropriate time. Therefore, it is crucial that we determine the exact moment where the low-speed system engagement will be the most optimal, not to risk any physical damage to the pod or the I-beam if the velocities are too high, so we should also determine a minimum value of velocity for which the low-speed system should not be engaged to avoid unnecessary risks.

Temperature I-beam: The eddy current braking systems work by generating currents in the I-beam, which will then produce the braking forces, but to achieve this a lot of heat will be dissipated and this could be a reason for concern. However, considering the I-beam is long and the halbach arrays will only face every section of the beam for a very short time, I don't think this short time will be enough to generate an amount of heat which would affect any part of the pod. Even if this is the case, testing should be performed in order to determine if the heat produced will be at appropriate levels or if something has to be done about it so as to improve safety, not only for the pod and its functionality but also for the people handling the I-beam and that have contact with it.

Handling magnets: When testing or building the braking systems, the magnets will have to be handled manually, and considering the large amounts of magnetization these have, we will need to be properly protected in order to avoid any risk of injuries or dangers. The magnets, when aligned with opposite poles will have a very strong attraction, so everyone in contact with the magnets must wear thick gloves to avoid injuries in case of having the hands between both magnets. The exact strength of the magnets will not be seen until we have them physically, but a good way to approach their use would be using a spacer to reduce their attraction and hence reduce the risk and make it easier to handle them.

The University of Manchester

General Risk Assessment Form

Date: 09/03/2022	Assessed by: Bassel Ezz	Checked / Validated* by: Rutvik Perepa, Dale Hamer	Location: Manchester, Delft, Hilversuum	Assessment ref no	Review date:
Task / premises: Bringing prototype into EHW					

Activity	Hazard	Who might be harmed and how	Existing measures to control risk	Risk rating	Result
Lifting or moving the prototype	Prototype contains magnets	Someone moving the prototype	Magnets will be safely stored or properly fixed. No large or strong magnets are used.	low	

3.6. Conclusion

The purpose of this section is to describe our brake design for the Final Showcase Document for EHW 2022. All the features and elements of our design to date have been included. In order to achieve our targets for competition, our plan is to perform the magnetic simulations and tests to validate the theory. We will also finalise work on the engagement mechanism and perform the necessary stress and vibrational analysis on the components. Finally, after obtaining accurate values for the mass of the system, the integration point with chassis will be finalised. Cost of manufacturing can therefore be estimated, although manufacturing will not be done this year.

4. Safety Compliance with the Rules & Requirements for Showcase

In order to comply with the Rules & Requirements for Showcase as established by the European Hyperloop Week group (EHW), below are described the measures and precautions taken by Hyperloop Manchester to fulfil the demands.

- In accordance with the provisions of rule **SC.1** in Section 5.1 of *Rules & Requirements for Showcase*, Hyperloop Manchester takes responsibility and declares the inexistence of any means of power generation system in the pod system in question to be showcased at EHW**.** To comply with this rule, the team will not implement a power source in the pod system during the showcase.

- In accordance with the provisions of rule **SC.2** in Section 5.1 of *Rules & Requirements for Showcase*, Hyperloop Manchester takes responsibility and declares the inexistence of any means of energy (this includes potential, kinetic, chemical, and electromagnetic energy) storage units, batteries or systems in the pod system to be showcased at EHW. To comply with this rule, any energy stored component will not be brought to the EHW site.

- In accordance with the provisions of rule **SC.3** in Section 5.1 of *Rules & Requirements for Showcase*, Hyperloop Manchester agrees to sign the EHW Terms and Conditions, in which they take full responsibility for any damage, incident or accident caused to or by their pod system.
- In accordance with the provisions of rule **SC.4** in Section 5.1 of *Rules & Requirements for Showcase*, Hyperloop Manchester commits to presenting a full and detailed list of the low power devices or appliances that are not part of the pod system and only intended for visual display or presentation purposes (e.g. LEDs, light, monitors). If any low power devices or appliances that are not part of the system are used, Hyperloop Manchester will solely use them if they have been previously approved by the EHW Committee. The predefined low power devices planned to be used so far on the site of EHW 2022, if any, are mentioned in this report in related sections.
- In accordance with the provisions of rule **SC.5** in Section 5.1 of *Rules & Requirements for Showcase*, Hyperloop Manchester agrees to follow and is liable to comply with all requirements listed in Section 9.3, *Transport, Storage and Lifting Requirements*. Hyperloop Manchester will provide their chosen transportation firm with all the guidelines necessary to adhere to the EHW regulations as specified.

Hereby, Hyperloop Manchester certifies that it has read and understood the Safety compliance with the Rules & Requirements for Showcase set by EHW for the 2022 competition and is responsible for any failed attempt to attain concurrence with the rules stated above.

Hyperloop Manchester Team 2021/22
Wednesday, 9th March 2022

5. References

[1] Kjmagnetics.com. 2021. *Halbach Arrays*. [online] Available at: <https://www.kjmagnetics.com/blog.asp?p=halbach-arrays> .

[2] Chen, Q., Tan, Y., Li, G., Li, J. and Mareels, I., 2017. DESIGN OF DOUBLE-SIDED LINEAR PERMANENT MAGNET EDDY CURRENT BRAKING SYSTEM. *Progress In Electromagnetics Research M*, 61, pp.61-73. Design of Double-Sided Linear Permanent Magnet Eddy Current Braking System

[3] Kratz, R. and Post, R., 2002. A null-current electro-dynamic levitation system. *IEEE Transactions on Appiled Superconductivity*, 12(1), pp.930-932.

[4] Post, R. and Ryutov, D., 2000. The Inductrack: a simpler approach to magnetic levitation. *IEEE Transactions on Appiled Superconductivity*, 10(1), pp.901-904.

[5] First4magnets.com. n.d. *Grades Of Neodymium Magnets | First4magnets.com*. [online] Available at: <https://www.first4magnets.com/tech-centre-i61/information-and-articles-i70/neodymium-magnet-information-i82/grades-of-neodymium-magnets-i92>.

[6] Fears, P., 2020. *Explaining Neodymium Magnet Strength - Bunting - Berkhamsted*. [online] Bunting - Berkhamsted. Available at: https://www.bunting-berkhamsted.com/explaining-neodymium-magnet-strength/.

[7] Parsons, R., Parsons, R. and profile, V., 2021. *The advantages and disadvantages of using a Halbach array with a BLDC (PMSM) motor*. [online] Things-in-motion.blogspot.com. Available at: <https://things-in-motion.blogspot.com/2018/12/the-advantages-and-disadvantages-of.html>.

[8] Yan, L., Zhang, L., Peng, J., Zhang, L. and Jiao, Z., 2016. Formulation of Magnetic Field. *Electromagnetic Linear Machines with Dual Halbach Array*, pp.17-34.